Journal of Photochemistry and Photobiology A: Chemistry 246 (2012) 60–66

Contents lists available at SciVerse ScienceDirect

Journal of Photochemistry and Photobiology A: Chemistry

journal homepage: www.elsevier.com/locate/jphotochem

Solvent effects on photosensitized splitting of thymine cyclobutane dimer by an attached phenothiazine

Hong-Mei Zhou[a], Wen-Jian Tang[a,*], Hong Zhang[a], Xiao-Xiang Li[a,b], Jun Li[a]

[a] School of Pharmacy, Anhui Medical University, Hefei 230032, PR China
[b] Anhui New Star Pharmaceutical Development Co., Ltd, Hefei 230088, PR China

ARTICLE INFO

Article history:
Received 14 May 2012
Received in revised form 24 July 2012
Accepted 25 July 2012
Available online 14 August 2012

Keywords:
DNA photorepair
Electron transfer
Cyclobutane pyrimidine dimer
Marcus theory
Solvent effect

ABSTRACT

The splitting quantum yields of the dimer by tethered chromophores exhibited different solvent effects. To further explore mechanism of the solvent effects, three covalently linked phenothiazine–dimer model compounds with a short linker, **1a**–**1c**, were prepared. It was observed that solvent effect on dimer-splitting efficiency for phenothiazine–dimer systems is contrary to that of the other chromophore–dimer systems. Calculated results based on the Marcus theory showed that phenothiazine systems with a lower driving force induced by a lower value of E_{ox} have a longer donor–acceptor distance between phenothiazine moiety and dimer unit, then gives a higher λ_s. Thus, back electron transfer would lie in the Marcus normal region for phenothiazine–dimer models, in which dimer-splitting is more efficient in higher polarity solvents. The value of redox potential between a donor and an acceptor should be a key leading to back electron transfer lying in the different Marcus regions and following two reverse solvent effects. Moreover, fluorescence spectra showed that the dual fluorescence gives a hint of charge-transfer complexes, and partial charge transfer would lead to lower splitting efficiency. However, some new insights into mechanisms of DNA photoreactivation mediated by photolyases were gained.

1. Introduction

There is great interest in the repair of damage to DNA caused by exposure to UV radiation. The UVB- or UVC-induced cyclobutane pyrimidine dimers (CPDs) are well known lesions in photobiology [1], whereas recent studies showed that CPDs can also be formed by UVA irradiation *via* a direct photochemical mechanisms due to the base pairing in DNA [2]. DNA photolyases can efficiently repair these photolesions by converting the dimerized pyrimidines to their monomeric form with the energy of visible light (Fig. 1). Experimental [3,4] and theoretical [5] investigations have provided evidence for the mechanisms of CPD photolyases. The enzymes transfer light energy, initially absorbed by an auxiliary chromophore, to a reduced flavin adenine dinucleotide ($FADH^-$) coenzyme. The excited $FADH^-$ donates an electron to the CPD to form the dimer radical anion, which cleaves spontaneously and then back electron transfer restores the original bases and the functional form of flavin ready for a new cycle of catalysis.

To unravel the mechanisms above in detail, several model compounds were used to mimic the virtually intramolecular electron transfer from the enzyme-bound sensitizer to the enzyme-bound dimer, such as a chromophore attached to a pyrimidine dimer unit. These model systems have offered useful insights into electron transfer and bond-breaking processes involved in photosensitized dimer splitting [6–11]. In the covalently linked chromophore–dimer model systems, the dimer splitting exhibited two reverse solvent effects on splitting efficiency. One is more efficient splitting in lower polarity solvents, which has been interpreted in terms of a possible slowing of the highly exothermic back electron transfer due to Marcus inverted behavior. The model systems with a short linker [8] showed such solvent dependence. Another is an increase in higher polarity solvents for model systems with a flexible and long liker [9].

In a previous work, we prepared five indole–dimer model compounds with different-length linkers [10] to investigate the origin of solvent dependence of the dimer-splitting effects on the length of the linkers. The length of linker plays an important role in the two reverse solvent effects on the quantum yield of dimer-splitting. For the model systems with a short linker, the increase in splitting efficiency in lower polarity solvents is fully identical to Rose et al.'s observations and interpretation. In the model systems with a long and flexible linker, the distance between a donor and an acceptor would become much less from a spreading to a U-shaped conformation with increasing solvent polarity because of

* Corresponding author. Tel.: +86 551 5161115; fax: +86 551 5161115.
E-mail address: tangwjster@gmail.com (W.-J. Tang).

1010-6030/$ – see front matter © 2012 Elsevier B.V. All rights reserved.
http://dx.doi.org/10.1016/j.jphotochem.2012.07.014

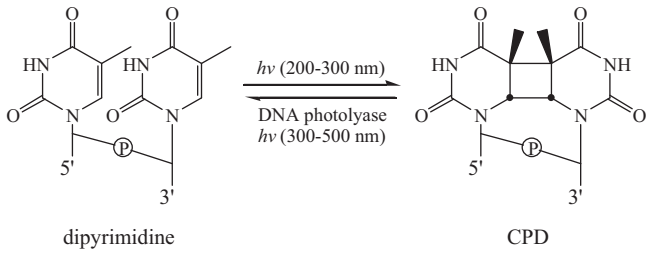

Fig. 1. UV-induced CPD photoproducts in DNA and their photorepair by DNA photolyases.

their hydrophobic interaction and the specific structure of dimer. And calculated results in terms of the Marcus theory also showed that the rate of back electron transfer would be slowed down with increasing solvent polarity, giving a more efficient splitting.

Recently, two reverse solvent effects were also observed in two classes of model compounds, covalently linked dimer– or oxetane–carbazole compounds, with a dimethylene or trimethylene group as a linker [11], however, in two model systems with the same linker and electron donor, the key difference is the one-electron reduction potential (E_{red}) of an acceptor (the dimer, −2.2 V, the oxetane, −1.8 to −2.0 V (SCE)). 0.2–0.4 V lower value of $-\Delta G_{bet}$ for oxetane-model systems would give a smaller driving force within the charge-separated species between the donor and the acceptor. This indicates that the oxetane systems have a longer donor–acceptor distance than the corresponding dimer systems, which would give a higher solvent-reorganization-energy (λ_s). Thus, a lower $-\Delta G_{bet}$ and a higher λ_s would lead back electron transfer to lie in the Marcus normal region for oxetane-model systems. Therefore, the value of redox potential between electron donor (chromophore moiety) and acceptor (dimer/oxetane) is a factor of determining the rate of back electron transfer.

In this work, we have prepared three covalently linked phenothiazine–dimer model compounds with a short linker **1a**–**1c** (Chart 1), and investigated the solvent dependence of dimer-splitting efficiency in various solvents. Although the trimethylene-bridged dimer enforces an almost planar ring, which is different to that of the unbridged dimer, the bridged dimer with *cis*–*syn* configure is easily prepared [8c]. Comparing with the carbazole–dimer model compounds **2a** and **2b**, experimental results have been analyzed according to Marcus theory [12]. For model systems with a short linker, solvent effect of dimer splitting in phenothiazine–dimer systems is contrary to that in nonphenothiazine–dimer systems. Furthermore, combining with the fluorescence quenching and solvent effects on dimer splitting, some new insights into the intramolecular electron transfer process in phenothiazine–dimer systems were gained.

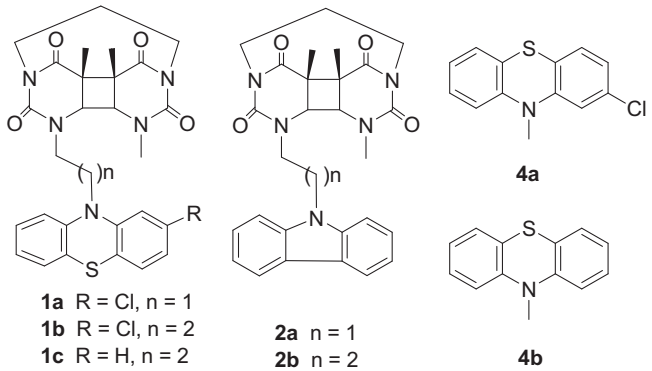

Chart 1.

2. Materials and methods

2.1. General methods

Melting points were uncorrected. All materials were obtained from commercial suppliers were used as received. Solvents of technical quality were distilled prior to use. Dimethylformamide (DMF) was dried overnight with K_2CO_3 and distilled. Tetrahydrofuran (THF) was dried with metal sodium and distilled before use, for the photosplitting measurements of model compounds. Acetonitrile and methanol were spectroscopic grade from commercial suppliers and used without further purification.

2.2. Measurement of steady-state fluorescence emission

Fluorescence emission spectra were measured at room temperature on a Shimadzu RF-spectrofluorophotomer. To determine the extent of fluorescence quenching, *Q*, fluorescence intensities ($F_{Ptz\text{-}D}$) of **1a**–**1c** were compared to that (F_{Ptz}) of the corresponding phenothiazine without a dimer attached respectively, that is $Q = 1 - F_{Ptz\text{-}D}/F_{Ptz}$. The concentrations of phenothiazine moiety of the phenothiazine–dimer models and the free phenothiazine, were controlled within 0.05 for absorbance at the wavelength of excitation 340 nm, and fluorescence intensities were normalized with the absorbance.

2.3. Measurement of splitting quantum yields of model compounds

To measure the quantum yields of dimer splitting of the model compounds, [(= (rate of dimer splitting)/(rate of photons absorbed)], all sample solutions (~5×10^{-5} M, 3 mL) were prepared in corresponding solvents and placed in quartz cuvettes with a Teflon stopper, then irradiated with 340 nm light from a fluorescence spectrometer with a 10 nm slit. The absorbance at 273 nm (A_{273}) and 340 nm (A_{340}) were recorded at certain intervals of time after irradiation. The extent of dimer splitting was measured by monitoring the increase in the absorbance at 273 nm (A_{273}) due to the regeneration of the thymine bases. The A_{273} change ((A_{273}) of the solution depends on the splitting extent of the model compounds. The plot of (A_{273} against the irradiation time (*t*, min) is well fitted as a straight line, where the slope of the straight line *B* reflected a splitting rate of the model compound. The intensity of the excitation light beam (I_0, unit: Einstein min^{-1}) was measured by ferrioxalate actinometry [13]. The intensity of light absorbed (I_a) by solution was calculated in term of Beer's law, $I_a = I_0(1 - 10^{A_{340}})$. The change in mole extinction coefficients ((($_{273}$) was obtained from UV absorption spectra of the model compounds and the fully splitting products. Above these values allowed the calculation of the quantum yield, (= BV_0/(($_{273}I_a$, wherein V_0 was the volume of irradiation solution, 3×10^{-3} L, the experimental error within 2%.

The quantum yields of splitting did not significantly change with and without N_2 bubbling prior to irradiation within experiment error of ±5%. Hence, the nondeaerated solution was employed in all measurements of quantum yield. To limit competition of absorption of irradiated light between model compounds and photoproducts, the splitting extent of model compounds was controlled within 10% in all the measurements of the quantum yield.

2.4. Characterization and synthesis of model compounds ***1a*–*1c***

Model compound 1a: K_2CO_3 (500 mg, 3.60 mmol), 1,2-dibromoethane (0.50 mL, 5.70 mmol) were added to a solution of *cis*, *syn*-thymine dimer **5** (184 mg, 0.60 mmol) in DMF (5 mL), and the reaction mixture was stirred at room temperature overnight. The 2-bromoethyl-dimer **6** was purified by extraction

and flash chromatography and obtained as a white powder (210 mg, 85%). **6** (104 mg, 0.25 mmol) was refluxed in acetone (10 mL) in the presence of NaI (100 mg, 0.67 mmol) for 5 h. The mixture was diluted with water and extracted with EtOAc twice. The organic layers were dried with Na_2SO_4, filtered, and concentrated *in vacuo*. The 2-iodoethyl-dimer product **7** was obtained as light yellow powder (92 mg, 80%). Cs_2CO_3 (163 mg, 0.50 mmol) and 2-chlorophenothiazine (70 mg, 0.30 mmol) were added to a solution of **7** (92 mg, 0.20 mmol) in DMF (2 mL) and the reaction was stirred overnight at room temperature. The mixture was diluted with water and extracted with EtOAc for 3 times. The organic layers were dried with Na_2SO_4, filtered, and concentrated *in vacuo*. The residue was subjected to flash chromatography (silica gel-*H*, petroleum ether/EtOAc = 1/0→1/4). The product was recrystallized from methanol as a white powder (20 mg, 18%). M.p. 196.4–201.8 °C; ^{1}H NMR (300 MHz, $CDCl_3$): δ = 1.29 (s, 3H, CH_3), 1.42 (s, 3H, CH_3), 1.62 (m, 1H), 2.38 (m, 1H), 2.87 (s, 3H, NCH_3), 2.97 (m, 1H), 3.68 (d, J = 7.0 Hz, 1H, CH), 3.92 (d, J = 7.2 Hz, 1H, CH), 3.89–4.36 (m, 7H), 6.86–7.23 (m, 7H, Ar—H); ^{13}C NMR (75 MHz, $CDCl_3$): δ = 18.4 (CH_3), 18.7 (CH_3), 22.9, 36.4, 41.7, 41.8, 43.1, 45.2, 50.8 (C), 51.7 (C), 60.0 (CH), 60.7 (CH), 116.1, 116.2, 123.4, 124.0, 124.2, 125.4, 128.1, 128.3, 128.7, 134.0, 144.2, 146.5, 151.9, 152.0, 170.2 (2C); HRMS (ESI-TOF) calculated for $C_{28}H_{29}ClN_5O_4S$ $[M+H]^+$ 566.1623, found 566.1617.

Model compound 1b: 2-Chlorophenothiazine (500 mg, 2.2 mmol) and 1,3-dibromopropane (4 mL, 39 mmol) were added to a suspension of 50% NaOH solution (5 mL), TBAB (0.15 g, 0.47 mmol) and toluene (5 mL), and the reaction was stirred at room temperature for 3.5 h. The mixture was diluted with water and extracted with EtOAc. The organic layers were dried with Na_2SO_4, filtered and concentrated *in vacuo*. The residue was purified by flash chromatography to obtain 1-(3-bromopropyl)-2-chlorophenothiazine as light yellow oil (160 mg, 21%). Sodium *t*-butoxide (40 mg, 0.4 mmol) was added to the solution of *cis*, *syn*-thymine dimer **5** (62 mg, 0.20 mmol) in DMF (3 mL) and the reaction was stirred at room temperature for 30 min. The above oil (160 mg, 0.45 mmol) was added, and then the stirring was resumed overnight at room temperature. The mixture was diluted with water and extracted with EtOAc. The organic layers were dried with Na_2SO_4, filtered, and concentrated *in vacuo*. The crude residue was subjected to flash chromatography (silica gel-*H*, EtOAc/petroleum ether = 3/2→3/1). The product was recrystallized from methanol as a white powder (83 mg, 72%). M.p. 157.4–159.6 °C; ^{1}H NMR (300 MHz, $CDCl_3$): δ = 0.78 (s, 3H, CH_3), 1.31 (s, 3H, CH_3), 1.55 (m, 1H), 2.18 (m, 1H), 2.34 (m, 1H), 2.72 (m, 1H), 2.89 (s, 3H, NCH_3), 3.64 (d, J = 7.2 Hz, 1H, CH), 3.76 (d, J = 7.2 Hz, 1H, CH), 3.80–4.25 (m, 7H), 6.89–7.28 (m, 7H, Ar—H); ^{13}C NMR (75 MHz, $CDCl_3$): δ = 17.6 (CH_3), 18.7 (CH_3), 22.9, 24.7, 36.4, 41.5, 41.8, 43.4, 45.3, 50.6 (C), 50.7 (C), 60.2 (CH), 60.8 (CH), 117.1, 117.2, 123.5, 124.1, 124.8, 126.1, 128.1, 128.3, 128.6, 134.2, 144.7, 146.5, 151.8, 152.1, 170.1, 170.5; ESI-MS: $[M+H]^+$ = 580.4; HRMS (ESI-TOF) calculated for $C_{29}H_{31}ClN_5O_4S$ $[M+H]^+$ 580.1780, found 580.1776.

Model compound 1c: Compound 1-(3-bromopropyl) phenothiazine was synthesized in a similar procedure through phenothiazine instead of 2-chlorophenothiazine, and obtained as light yellow oil (150 mg, 23%). Sodium *t*-butoxide (40 mg, 0.4 mmol) was added to the solution of *cis*, *syn*-thymine dimer **5** (80 mg, 0.26 mmol) in DMF (4 mL) and the reaction was stirred at room temperature for 30 min. The above oil (150 mg, 0.47 mmol) was added, and then the stirring was resumed overnight at room temperature. The mixture was diluted with water and extracted with EtOAc. The organic layer was dried with Na_2SO_4, filtered, and concentrated *in vacuo*. The residue was subjected to flash chromatography with *silica-H* absorbent ($CHCl_3$→EtOAc). The product was recrystallized from methanol as a white powder (110 mg, 78%). M.p. 194.2–197.8 °C; ^{1}H NMR (300 MHz, $CDCl_3$): δ = 0.70 (s, 3H, CH_3), 1.30 (s, 3H, CH_3), 1.54 (m, 1H), 2.05–2.43 (m, 3H), 2.88 (s, 3H, NCH_3), 2.76 (m, 1H), 3.65 (d, J = 7.0 Hz, 1H, CH), 3.82 (d, J = 7.2 Hz, 1H, CH), 3.83–4.18 (m, 7H), 6.91–7.29 (m, 8H, Ar—H); ^{13}C NMR (75 MHz, $CDCl_3$): δ = 17.3 (CH_3), 18.5 (CH_3), 22.7, 24.6, 36.2, 41.7, 41.8, 45.7, 46.4, 50.4 (C), 50.5 (C), 59.9 (CH), 60.6 (CH), 116.8 (4C), 123.4 (2C), 126.3, 127.9 (4C), 146.5, 151.7, 152.0, 170.1, 170.4; HRMS (ESI-TOF) calculated for $C_{29}H_{32}N_5O_4S$ $[M+H]^+$ 546.2168, found 546.2167.

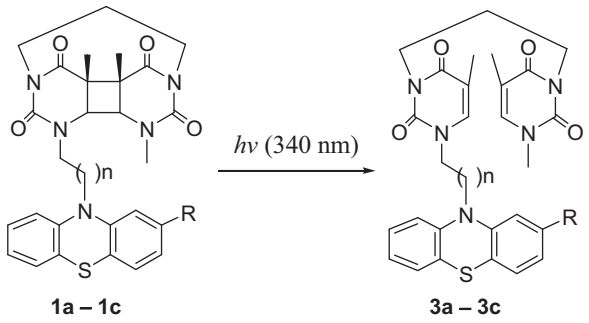

Fig. 2. Photosensitized splitting reactions of dimer unit of model compounds under irradiation with 340 nm light.

3. Results and discussion

3.1. Synthesis of the model compounds *1a–1c*

Three model compounds were synthesized from the *cis–syn* thymine dimer [10] *via* the routes depicted in Scheme 1. The *N*-alkylation of *cis–syn* thymine dimer **5** was reacted with 1,2-dibromoethane in DMF to yield 2-bromoethyl-dimer **6**, which was converted to 2-iodoethyl-dimer **7** as light yellow powder by the Finkelstein reaction. The model compound **1a** was obtained by the reaction of **7** with 2-chlorophenothiazine in the presence of cesium carbonate. The model compounds **1b** and **1c** were prepared from *cis–syn* thymine dimer **5** alkylated with the corresponding 1-(3-bromopropyl)-2-chloro-phenothiazine and 1-(3-bromopropyl) phenothiazine in 72% and 78% yield respectively. The *N*-alkylation of phenothiazine (or 2-chlorophenthiazine) with excessive 1,3-dibromopropane was carried out through tetrabutyl ammonium bromide (TBAB) as phase-transfer catalyst in toluene/water solvent. The synthesis of compounds **4a**, **4b** and **3c** is presented in Supporting Information.

3.2. Photosplitting properties of the model compounds

The model compounds **1a–1c** in methanol solution was irradiated with a 340 nm light beam from a fluorescence spectrometer with a 125 W Xe lamp passed through a monochromator. Analysis of the photolysis mixture by reverse-phase HPLC confirmed that the model compounds react cleanly to give **3a**, **3b** and **3c** from **1a**, **1b** and **1c** respectively (Fig. 2).

Furthermore, the expected photoproduct **3c** was synthesized and identified by NMR and HPLC co-injection. A representative set of HPLC chromatograms showing the simultaneous splitting of model **1c** into **3c** was depicted in Fig. 3. Obviously, the splitting reaction of model **1c**, with retention time of 5.2 min, to the photosplitting product **3c**, with retention time of 5.7 min, is clean conversion as no other products could be detected.

3.3. Fluorescence emission spectra

Fig. 4 showed the fluorescence emission spectra of models **1a–1c** and the free phenothiazine (either *N*-methyl-2-chlorophenothiazine **4a** or *N*-methyl-phenothiazine **4b**) in

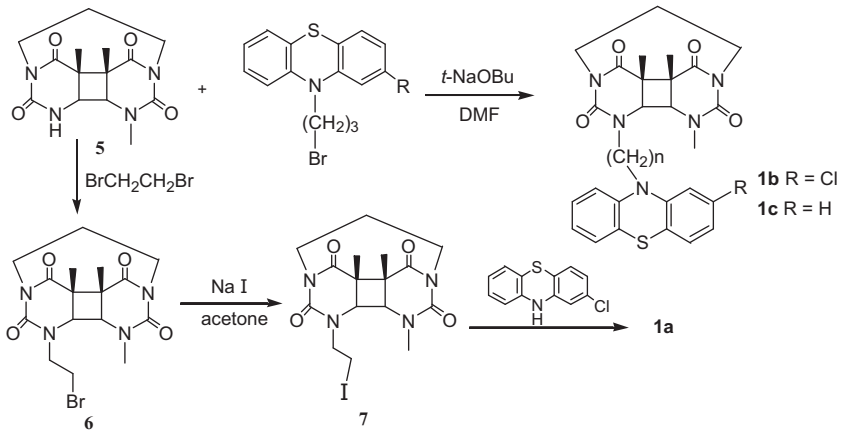

Scheme 1.

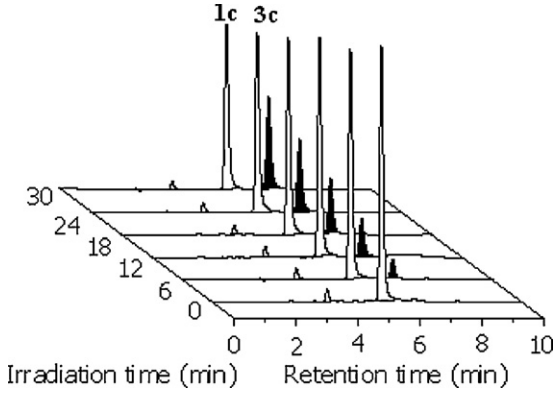

Fig. 3. Typical HPLC chromatograms obtained after 0, 6, 12, 18, 24 and 30 min of irradiation of **1c** in methanol (3 mL, 5×10^{-5} M) with 340 nm light. Assay conditions: C_{18} reverse-phase column, methanol:water (85:15), detection at 273 nm. Retention times: 5.2 min (model **1c**), 5.7 min (photoproduct **3c**).

MeCN/H_2O (40:60) and methanol at room temperature. A dual fluorescence emission was observed in the proximity of 390 and 460 nm and the ratio of the intensities of the "blue" and "red" emission bands varied not only with substituent but also with solvent polarity. The red-shift fluorescence may be an emission of the charge-transfer complexes [14], and the model compounds display different dual fluorescence. Comparing to the dual fluorescence of the free phenothiazine **4a** (or **4b**), the dual fluorescence intensities of model **1b** became both weaker, whereas those of models **1a** and **1c** exhibited different changes, the blue emission increasing and the red one decreasing, which implied that more charge-transfer in models **1a** and **1c** occurs. Therefore, fluorescence quenching was mainly observed for model **1b**, while both charge transfer and fluorescence quenching existed for models **1a** and **1c**.

The fluorescence quenching of phenothiazine moiety is not a result of absorption of exciting light by the dimer, because dimer has no absorption above 300 nm. Additionally, there is no overlap between emission spectra of the free phenothiazine and absorption spectra of the thymine dimer (not shown), thus, singlet–singlet energy transfer is an improbable pathway of fluorescence quenching in the model compounds. Hence, an intramolecular electron transfer from the excited phenothiazine moiety to the dimer unit should be reliable pathway of fluorescence quenching, and the degree of fluorescence quenching for model **1b** can reflect the efficiency (Q) of forward electron transfer reaction [8c,9e].

According to the Rehm–Weller equation (Eq. (1)) [15], free energy change (ΔG_{fet}) for the proposed electron-transfer reactions from the excited phenothiazine moiety to the dimer unit can be estimated.

$$\Delta G_{fet}(\text{eV}) = E_{ox}(\text{D}) - E_{red}(\text{A}) + \Delta E_{coul} - \Delta E_{0,0} \quad (1)$$

$$\Delta E_{coul}(\text{eV}) = \frac{e}{4\pi\varepsilon_0 a}\left(\frac{1}{\varepsilon} - \frac{2}{37.5}\right) \quad (2)$$

where E_{ox} and E_{red} are potentials for one-electron oxidation of a donor (*N*-methylphenothiazine, 0.73 V (SCE), almost E_{ox} value for **4a** due to the near values of chlorpromazine (0.78 V) and promazine (0.71 V) with a same 10-substituent) [16] and one-electron reduction of an acceptor (dimer, −2.20 V (SCE) [17]), respectively.

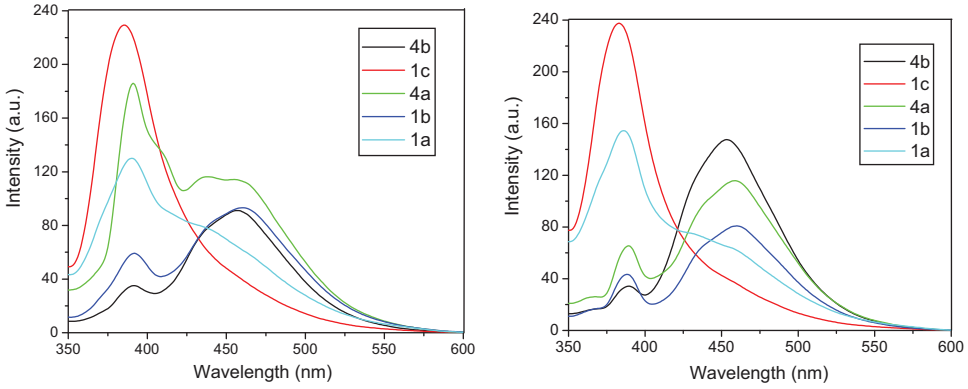

Fig. 4. Fluorescence emission spectra of model compounds **1a–1c** and the free phenothiazine **4a**, **4b**, in MeCN/H_2O (40:60) (left) and in methanol (right), upon excitation at 340 nm.

Table 1
Free energy change (ΔG_{fet}, eV) of forward electron transfer reactions for different model systems in three solvents.

Solvent	Carbazole–dimer[a]	Phenothiazine–dimer[b]	Phenothiazine–dimer[c]
THF	+0.33	−0.07	+0.42
MeOH	−0.13	−0.38	+0.18
Water	−0.15	−0.42	+0.14

[a] From Ref. [8].
[b] Calculation with in various solvents and E_{ox} = 0.73 V of *N*-methylphenothiazine.
[c] Calculation if the excitation wavelength is 460 nm.

Table 2
The splitting quantum yield (Φ) of models **1a–1c** and fluorescence quenching extent (Q) of model **1b** in various solvents.

Solvents	Φ[a] for compounds					
	1a	**1b**	**1b** (Q)	**1c**	**2a**[c]	**2b**[c]
THF	[b]	[b]	0.83	[b]	[b]	[b]
Acetonitrile	0.004	0.022	<0	0.006	[b]	[b]
Methanol	0.018	0.013	0.47	0.018	0.101	0.089
MeCN/H_2O (80:20)	0.013	0.048	0.23	0.013	0.089	0.088
MeCN/H_2O (60:40)	0.028	0.056	0.28	0.016		
MeCN/H_2O (40:60)	0.029	0.090	0.40	0.023	0.074	0.084
MeCN/H_2O (25:75)	0.029	0.105	0.53	0.047		

[a] Average of two determinations; 10 nm bandwidth.
[b] No splitting detected.
[c] From Ref. [11]. Estimated error in Φ = ±10%.

ΔE_{coul} and $\Delta E_{0,0}$ are the Coulomb term and the energy level of the excited state, respectively. The latter can be obtained from the fluorescence peaks of phenothiazine–dimer model compounds in the corresponding solvents. ε, a are the static dielectric constant of a solvent and the center-to-center distance between a donor and an acceptor, respectively, and $\varepsilon_0 = 8.854 \times 10^{-12}\,C\,V^{-1}\,m^{-1}$.

If a = 6 Å for model **1b** with a trimethylene, values of free energy changes (ΔG_{fet}) can be calculated, as listed in Table 1. The values of ΔG_{fet} in 460 nm band in all solvents are no more than zero. These results showed that forward electron transfer is thermodynamically possible in the blue band in polar solvents, but impossible in the red band in all solvents, and the ΔG_{fet} in THF is unfavorable for the dimer splitting. The fluorescence quenching of model **1b** occurs in polar solvents. Comparing with fluorescence intensity of the free phenothiazine in the blue band in corresponding solvents, fluorescence quenching (Q) of the phenothiazine moiety for model **1b** was obtained in various solvents, and listed in Table 2. Model **1b** has medium fluorescence quenching extents in polar solvents, whereas, the Q values of models **1a** and **1c** cannot be calculated due to the change of dual fluorescence. In THF, the Q value of model **1b** cannot also be observed due to the similar fluorescence emission to **1a**.

The photophysical and photochemical processes of **1a–1c** (represented as Ch–D) are illuminated with a simple mechanistic scheme (Fig. 5). Upon irradiation with light, the phenothiazine moiety absorbs a photon to produce the excited state $^1Ch^*$–D. The excited state has the following relaxation pathways: fluorescence (k_f or k_f'), internal conversion (k_{ic}), charge transfer (k_{CT}) to lower excited state ($^1Ch^*$–D′) and electron transfer to a covalently linked dimer (k_{fet}). The charge-separated species ($Ch^{\bullet+}$–$D^{\bullet-}$) formed by the electron transfer, undergoes two competitive processes: splitting (k_{spl}) to produce M′ and $Ch^{\bullet+}$–$M^{\bullet-}$ (it then becomes Ch–M by charge combination) and back electron transfer (k_{bet}) to return to the starting substrate. In these processes, k_{fet} and k_{spl} contribute to the observed splitting quantum yield (Φ) of dimer, while k_{bet}, k_f, k_f', k_{ic} and k_{CT} reduce the quantum efficiency.

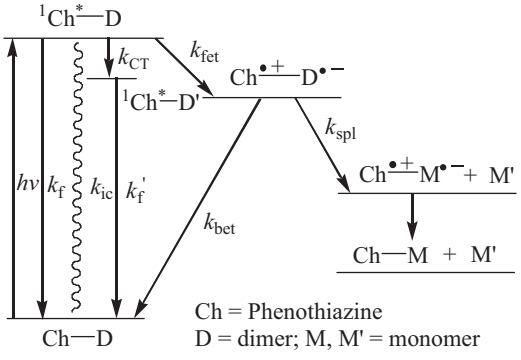

Fig. 5. Photophysical and photochemical processes of model compounds.

3.4. Splitting quantum yields of model compounds *1a–1c*

To obtain the observed quantum yields (Φ) of the model compounds, all sample solutions were prepared in seven solvents, THF, acetonitrile, methanol, acetonitrile/water (80:20), (60:40), (40:60), (25:75) mixture, placed in cuvettes with a Teflon stopper, and then irradiated with 340 nm light from a fluorescence spectrometer. After certain time intervals, the absorption spectra of the irradiated solution were recorded with a UV–vis spectrometer. The intensity of the light beam was measured for three times during the sample measurement, and the average value was employed. Based on the results, the observed quantum yields of dimer splitting of model compounds are calculated and listed in Table 2.

In the lower-polar solvent, THF, although the fluorescence quenching was observed in the model compounds, the thermodynamic data showed that ΔG_{fet} is unfavorable for dimer splitting, thus no subsequent splitting reaction takes place. The data in Table 2 show that the quantum yields of dimer splitting of **1a–1c** are strong solvent-dependent. The values of Φ decrease with solvent polarity, range from 0.029 in MeCN—H_2O (25:75) to 0.004 in acetonitrile for **1a**, 0.105 in MeCN—H_2O (25:75) to 0.013 in methanol for **1b**, and 0.047 in MeCN—H_2O (25:75) to 0.006 in acetonitrile for **1c**. Hence, the efficiencies of dimer splitting are enhanced in high polarity solvents. In the previous chromophore–dimer model systems with a short linker, the splitting quantum yields of dimer unit have exhibited an increase in lower polarity solvents. Therefore, in the covalently linked chromophore–dimer model systems with a short linker, two reverse solvent effects have been observed. One

is that the splitting quantum yield is a positive correlation with solvent polarity for phenothiazine–dimer systems, which is more efficient splitting in higher polarity solvents. Another is a negative correlation for the other chromophore–dimer systems with a short linker.

In the covalently linked indole–dimer models with different-length linkers [10], we have observed two reverse solvent effects on the splitting efficiency and demonstrated that the two reverse solvent effects derive from the difference in the conformational change between short- and long-linker compounds. Recently, Wu and Song [11] prepared two classes of covalently linked dimer– or oxetane–carbazole model compounds and confirmed that the reverse solvent effects derive from back electron transfer in splitting process lying in the different Marcus regions, and back electron transfer lies in the Marcus inverted region for dimer-model systems and the normal region for oxetane-model systems.

In the dimer-containing model systems with a short linker [6–11], the phenothiazine–dimer models in this work revealed a contrary solvent effect to the other chromophore–dimer model systems. In the electron-transfer reaction process, back electron transfer, which is a key leading to decrease splitting efficiencies of model compounds, should be the key factor controlling the two reverse solvent effects [18]. Comparing to the recently reported carbazole–dimer systems (**2a**, **2b**) [11], we would discuss the observed contrary solvent effect in this work. According to Marcus' theory [12], the rate of electron transfer is expressed by,

$$k_{bet} = A' \exp\left[\frac{-(\Delta G + \lambda_s)^2}{4\lambda_s k_B T}\right] \quad (3)$$

The equation is allowed to evaluate the rate of back electron transfer in the photosensitized splitting reaction of model compounds. The free energy of activation (G^+) can be obtained from the change of free energy (ΔG) and the solvent reorganization energy (λ_s) for back electron transfer. The former is the energy level of the charge-separated state ($Ch^{\bullet+}$–$D^{\bullet-}$), which can be estimated by using thermodynamic redox potentials. The free energy difference between the charge transfer state and the ground state is given by Eq. (4),

$$\Delta G_{bet} = E_{ox} - E_{red} + \Delta E_{coul} \quad (4)$$

The solvent reorganization energy of back electron transfer (λ_s) can be estimated using the equation [19] as follows,

$$\lambda_s = \frac{e}{4\pi\varepsilon_0}[(2r_D)^{-1} + (2r_A)^{-1} - (R_{DA})^{-1}](\varepsilon_{op}^{-1} - \varepsilon_s^{-1}) \quad (5)$$

where r_D and r_A are the ionic radii of the donor and the acceptor, respectively, and R_{DA} is the distance between a donor and an acceptor, that is a in Eq. (2). While ε_{op} and ε_s are the optical and static dielectric constant of the solvent, respectively, with $\varepsilon_{op} \approx n^2$, n being the solvent refractive index.

According to Marcus' theory (Eqs. (3)–(5)), the terms influencing the values of $-\Delta G_{bet}$ and λ_s are ΔE_{coul}, R_{DA}, and $(\varepsilon_{op}^{-1} - \varepsilon_S^{-1})$ in different solvents. Among them, two key factors are dielectric constant of solvents and the center-to-center distance between a donor and an acceptor, R_{DA} (a). Because of the models **1b** and **2b** with the same linker, electron acceptor and similar tricyclic donors, the center-to-center distance, R_{DA} (a), is taken as a constant. The conformation change of model compounds in different solvents would give different values of R_{DA} (a), thus, we can estimate solvent effects on ΔE_{coul} and $(\varepsilon_{op}{}^{-1} - \varepsilon_s{}^{-1})$ as well as $-\Delta G_{bet}$ and λ_s. However, the difference of the values of ΔE_{coul}, $(\varepsilon_{op}{}^{-1} - \varepsilon_s{}^{-1})$ or λ_s in an identical solvent for models **1b** and **2b** are neglected, the key difference in dimer-containing model systems is one-electron oxidation potential of the donor. A higher value of E_{ox} would give a larger value of $-\Delta G_{bet}$, when $-\Delta G_{bet} > \lambda_s$, as the polarity of the solvent decreases, the back electron transfer would lie in the so-called Marcus inverted region, in which back electron transfer in low-polar media would become so exothermic as slow the back electron transfer and lead to an efficient splitting, i.e., the splitting efficiency increases with decreasing solvent polarity. With the value of E_{ox} decreasing, a smaller value of $-G_{bet}$ would lead $-\Delta G_{bet} < \lambda_s$, then back electron transfer lies in the Marcus normal region, and a contrary varying trend to the situation above is expected. Therefore, back electron transfer lying in two Marcus regions would reveal two reverse solvent effects on the splitting quantum yield.

Based on the probability of back electron transfer lying in different Marcus regions, we would explain the two reverse solvent effects observed in the chromophore–dimer model systems. The one-electron oxidation potential of the donor, E_{ox}, of *N*-ethylcarbazole and *N*-alkyl-2-chlorophenothiazine is 1.12 V and 0.73 V vs saturated calomel electrode (SCE), respectively. The value of E_{ox} for phenothiazine–dimer systems is lower by 0.39 V than that for carbazole–dimer systems. Additionally, phenothiazine systems with a larger driving force of forward electron transfer (ΔG_{fet}, lie in Marcus normal region) have a lower value of Q than carbazole systems. This indicates that phenothiazine systems have a longer donor–acceptor distance than carbazole systems, then gives a higher λ_s. Hence, combining 0.39 V lower value of $-\Delta G_{bet}$ and a higher λ_s indicates that it is possible that back electron transfer would lie in the Marcus normal region for phenothiazine systems, and the inverted region for carbazole systems. Whether in dimer– and oxetane–carbazole systems with the same linker and electron donor or in chromophore-containing dimer systems with the same linker and electron acceptor, a lower redox potential is a key leading to back electron transfer lying in the different Marcus regions and following two reverse solvent effects.

However, the splitting quantum yields of model **1a** with a dimethylene linker were much lower than those of model **1b** with a trimethylene linker in an identical solvent, which is different to the other dimer-containing models, *e.g.* **2a** and **2b** (Table 2). The splitting efficiency of model **1c** was also lower than that of model **1b** with the same linker. The charge-transfer complexes (k_{CT}), as one of the relaxation pathways of the excited state in Fig. 5, could lead to less electron transfer to a covalently linked dimer (k_{fet}) and lower splitting efficiency. The larger change of dual fluorescence of models **1a** and **1c** showed more charge-transfer complexes and less forward electron transfer. Therefore, lower splitting efficiency of models **1a** and **1c** may be the result of partial charge-transfer that exists in the excited state only shifts the emission but does not automatically yields dimer splitting.

4. Conclusions

In summary, two reverse solvent effects have been observed from the splitting quantum yields of the chromophore–dimer model systems with a short linker, and it has been rationalized based on Marcus theory. One solvent effect is an increase in the splitting efficiency in higher polarity solvents for models **1a**–**1c**, and another is more efficient splitting in solvents of lower polarity for model compounds, the dimer by the attached other chromophore, such as carbazole, indole, arylamine, *etc.* Due to the larger difference in values of E_{ox} of electron donors between phenothiazine systems and non-phenothiazine systems, back electron transfer in splitting process would lie in the different Marcus regions. Back electron transfer lies in the Marcus normal region for phenothiazine–dimer models with much lower value of E_{ox} and the Marcus inverted region for non-phenothiazine models. Moreover, fluorescence spectra showed that the red-shift fluorescence may be an emission of the charge-transfer complexes and partial charge transfer would lead to the lower splitting quantum yields of models **1a** and **1c**.

It can be deduced that in enzyme–substrate complex the flavin ring binds CPD lesions in the polar pocket by a short distance to increase the efficiency of catalytic repair [20], and the redox potentials of flavoproteins may be tuned by the polarity of binding pocket, FAD conformation and hydrogen bonding, *e.g.* the active flavin accommodates butterfly-like ring buckle as the electron in and out of FADH [21].

Acknowledgments

We would like to acknowledge helpful discussions with Qin-Hua Song (University of Science & Technology of China). The authors are grateful for the financial support by the National Natural Science Foundation of China (Grant No. 20802003), Anhui Province and China Postdoctoral Science Foundation (Grant No. 20100470823).

References

[1] (a) J. Cadet, P. Vigny, in: H. Morrison (Ed.), Bioorganic Photochemistry. Vol. 1: The Photochemistry of Nucleic Acids, Wiley & Sons, New York, 1990, pp. 1–272;
(b) E.C. Friedberg, G.C. Walker, W. Siede, DNA Repair and Mutagenesis, ASM Press, Washington, DC, 1995;
(c) J. Cadet, M. Berger, T. Douki, B. Morin, S. Raoul, J.-L. Ravanat, S. Spinelli, Biological Chemistry 378 (1997) 1275–1286;
(d) W.J. Schreier, T.E. Schrader, F.O. Koller, P. Gilch, C.E. Crespo-Hernández, V.N. Swaminathan, T. Carell, W. Zinth, B. Kohler, Science 315 (2007) 625–629.

[2] (a) Y. Jiang, M. Rabbi, M. Kim, C. Ke, W. Lee, R.L. Clark, P.A. Mieczkowski, P.E. Marszalek, Biophysical Journal 96 (2009) 1151–1158;
(b) S. Mouret, C. Philippe, J. Gracia-Chantegrel, A. Banyasz, S. Karpati, D. Markovitsi, T. Douki, Organic and Biomolecular Chemistry 8 (2010) 1706–1711;
(c) A. Banyasz, I. Vayá, P. Changenet-Barret, T. Gustavsson, T. Douki, D. Markovitsi, Journal of the American Chemical Society 133 (2011) 5163–5165.

[3] (a) A. Sancar, Biochemistry 33 (1994) 2–9;
(b) A. Sancar, Chemical Reviews 103 (2003) 2203–2237.

[4] (a) Y.-T. Kao, C.L. Saxena, J. Wang, A. Sancar, D. Zhong, Proceedings of the National Academy of Sciences of the United States of America 102 (2005) 16128–16132;
(b) C.-W. Chang, L. Guo, Y.-T. Kao, J. Li, C. Tan, T. Li, C. Saxena, Z. Liu, L. Wang, A. Sancar, D. Zhong, Proceedings of the National Academy of Sciences of the United States of America 107 (2010) 291–296;
(c) Z. Liu, C. Tan, X. Guo, Y.-T. Kao, J. Li, L. Wang, A. Sancar, D. Zhong, Proceedings of the National Academy of Sciences of the United States of America 108 (2011) 14831–14836.

[5] (a) F. Masson, T. Laino, I. Tavernelli, U. Rothlisberger, J. Hutter, Journal of the American Chemical Society 130 (2008) 3443–3450;
(b) F. Masson, T. Laino, U. Rothlisberger, J. Hutter, ChemPhysChem 10 (2009) 400–410;
(c) A.A. Hassanali, D. Zhong, S.J. Singer, Journal of Physical Chemistry B 115 (2011) 3848–3859.

[6] (a) T.P. Begley, Accounts of Chemical Research 27 (1994) 394–401;
(b) P.F. Heelis, R.F. Hartman, S.D. Rose, Chemical Society Reviews 24 (1995) 289–297;
(c) K. Heil, D. Pearson, T. Carell, Chemical Society Reviews 40 (2011) 4271–4278.

[7] (a) R. Epple, T. Carell, Journal of the American Chemical Society 121 (1999) 7318–7329;
(b) W.J. Tang, Q.H. Song, H.B. Wang, J.Y. Yu, Q.X. Guo, Organic and Biomolecular Chemistry 4 (2006) 2575–2580;
(c) Q.H. Song, W.J. Tang, X.B. Ji, H.B. Wang, Q.X. Guo, Chemistry: A European Journal 13 (2007) 7762–7770.

[8] (a) S.-T. Kim, R.F. Hartman, S.D. Rose, Photochemistry and Photobiology 52 (1990) 789–794;
(b) S.-T. Kim, S.D. Rose, Journal of Photochemistry and Photobiology B 12 (1992) 179–191;
(c) D.G. Hartzfeld, S.D. Rose, Journal of the American Chemical Society 115 (1993) 850–854.

[9] (a) T. Young, S.-T. Kim, J.R. Van Camp, R.F. Hartman, S.D. Rose, Photochemistry and Photobiology 48 (1988) 635–641;
(b) R. Epple, E.-U. Wallenborn, T. Carell, Journal of the American Chemical Society 119 (1997) 7440–7451;
(c) T. Carell, R. Epple, European Journal of Organic Chemistry (1998) 1245–1258;
(d) J. Butenandt, R. Epple, E.-U. Wallenborn, A.P. Eker, E.-U. Gramlich, T. Carell, Chemistry: A European Journal 6 (2000) 62–72;
(e) Q.H. Song, W.J. Tang, X.M. Hei, H.B. Wang, Q.X. Guo, S.Q. Yu, European Journal of Organic Chemistry (2005) 1097–1106.

[10] W.J. Tang, Q.X. Guo, Q.H. Song, Journal of Physical Chemistry B 113 (2009) 7205–7210.

[11] Q.Q. Wu, Q.H. Song, Journal of Physical Chemistry B 114 (2010) 9827–9832.

[12] (a) R.A. Marcus, Journal of Chemical Physics 24 (1956) 966–978;
(b) R.A. Marcus, N. Sutin, Biochimica et Biophysica Acta 811 (1985) 265–322.

[13] S.L. Murov, I. Carmichael, G.L. Hug, Handbook of Photochemistry, 2nd ed., Marcel Dekker Inc., New York, 1993.

[14] (a) A. Stockmann, J. Kurzawa, N. Fritz, N. Acar, S. Schneider, J. Daub, R. Engl, T. Clark, Journal of Physical Chemistry A 106 (2002) 7958–7970;
(b) N. Acar, J. Kurzawa, N. Fritz, A. Stockmann, C. Roman, S. Schneider, T. Clark, Journal of Physical Chemistry A 107 (2003) 9530–9541.

[15] D. Rehm, A. Weller, Israel Journal of Chemistry 8 (1970) 259–271.

[16] (a) B.A. Kowert, L. Marcoux, A.J. Bard, Journal of the American Chemical Society 94 (1972) 5538–5550;
(b) E. Pelizzetti, E. Mentasti, Inorganic Chemistry 18 (1979) 583–588.

[17] M.R. DeFelippis, C.P. Murthy, F. Broitman, D. Weinraub, M. Faraggi, M.H. Klapper, Journal of Physical Chemistry 95 (1991) 3416–3419.

[18] Y.-T. Kao, Q.H. Song, C. Saxena, L. Wang, D. Zhong, Journal of the American Chemical Society 134 (2012) 1501–1503.

[19] (a) R.A. Marcus, Canadian Journal of Chemistry 37 (1959) 155–163;
(b) R.A. Marcus, Annual Review of Physical Chemistry 15 (1964) 155;
(c) A.A. Weller, Zeitschrift fur Physikalische Chemie (Muenchen, Germany) 133 (1982) 93–98.

[20] (a) H.-W. Park, S.-T. Kim, A. Sancar, J. Deisenhofer, Science 268 (1995) 1866–1872;
(b) J. Antony, D.M. Medvedev, A.A. Stuchebrukhov, Journal of the American Chemical Society 122 (2000) 1057–1065.

[21] (a) A. Mees, T. Klar, P. Gnau, U. Hennecke, A.P. Eker, T. Carell, L.-O. Essen, Science 306 (2004) 1789–1793;
(b) A.K. Murphy, M. Tammaro, F. Cortazar, Y.M. Gindt, J.P.M. Schelvis, Journal of Physical Chemistry B 112 (2008) 15217–15226.